

Seventy Years of Radar and Communications

The road from separation to integration



©SHUTTERSTOCK.COM/TRIFF

Radar and communications (R&C) as key utilities of electromagnetic (EM) waves have fundamentally shaped human society and triggered the modern information age. Although R&C had been historically progressing separately, in recent decades, they have been converging toward integration, forming integrated sensing and communication (ISAC) systems, giving rise to new highly desirable capabilities in next-generation wireless networks and future radars. To better understand the essence of ISAC, this article provides a systematic overview of the historical development of R&C from a signal processing (SP) perspective. We first interpret the duality between R&C as signals and systems, followed by an introduction of their fundamental principles. We then elaborate on the two main trends in their technological evolution, namely, the increase of frequencies and bandwidths and the expansion of antenna arrays. We then show how the intertwined narratives of R&C evolved into ISAC and discuss the resultant SP framework. Finally, we overview future research directions in this field.

Introduction

Background and motivation

Since the 20th century, the development of human civilization has relied largely upon the exploitation of EM waves. Governed by Maxwell's equations, EM waves are capable of traveling over large distances at the speed of light, which makes them a perfect information carrier. In general, one may leverage EM waves to acquire information on physical targets, including range, velocity, and angle, and to efficiently deliver artificial information, e.g., texts, voices, images, and videos, from one point to another. Among many applications, EM waves have enabled information acquisition and delivery, which form the foundation of our modern information era and have given rise to the proliferation of R&C technologies.

While the existence of EM waves was theoretically predicted by Maxwell in 1865 and experimentally verified by Hertz in 1887, the waves' capability of carrying information to travel long distances was not validated until Marconi's transatlantic

wireless experiment in 1901 [1]. The successful reception of the first transatlantic radio signal marked the beginning of the great information era. From then on, communication technology rapidly grew thanks to the heavy demand for intelligence, intercept, and cryptography technologies during the two world wars. It is generally difficult to identify a precise date for the birth of radar. Some of the early records show that the German inventor Christian Hülsmeyer was able to use radio signals to detect distant metallic objects as early as 1904. In 1915, the British radar pioneer Robert Watson Watt employed radio signals to detect thunderstorms and lightning. The R&D of modern radar systems was not carried out until the mid-1930s. The term *radar* was first used by the U.S. Navy as an acronym for “radio detection and ranging” in 1939.

Despite the fact that both technologies originated from the discoveries of Maxwell and Hertz, R&C have been largely treated as two separate research fields, due to different constraints in their respective applications, and were therefore independently investigated and developed for decades. Historically, the technological evolution of R&C follows two main trends: 1) from low frequencies to higher frequencies and larger bandwidths [2] and 2) from single-antenna to multiantenna and even massive antenna arrays [3], [4]. With recent developments, the combined use of large antenna arrays and millimeter-wave (mm-wave)/terahertz (THz) band signals results in striking similarities among R&C systems in terms of hardware architecture, channel characteristics, and SP methods. Hence, the boundary between R&C is becoming blurred, and hardware and spectrum convergence has led to a design paradigm shift, where the two systems can be codesigned for efficiently utilizing resources, offering tunable tradeoffs and unprecedented synergies for mutual benefits. This line of research is typically referred to as *ISAC*, and is applicable in numerous emerging areas, including vehicular networks, Internet of Things (IoT) networks, and activity recognition [5], [6]. Over the past decade, ISAC has been well recognized as a key enabling technology for both next-generation wireless networks and radar systems [5]. Given the potential of ISAC, a deeper understanding of the various connections and distinctions between R&C, and learning from how they evolved from separation to integration, is important for inspiring future research.

In Figure 1 we summarize key milestones achieved in R&C history, which are split into four categories with different markers, namely, the individual R&C technologies, general technologies that are useful for both, and ISAC technologies. In the remainder of the article, we discuss how these key techniques facilitate the development of R&C and ISAC systems.

Summary and organization of the article

In this article, we provide a systematic overview of the development and key milestones achieved in the history of R&C from an SP perspective. We commence by introducing the fundamental principles and SP theories of both R&C. We then present the spectrum engineering of R&C, namely, from narrowband to wideband and from single-carrier to multicarrier systems. Furthermore, we elaborate on the expansion of R&C systems’ antenna arrays, i.e.,

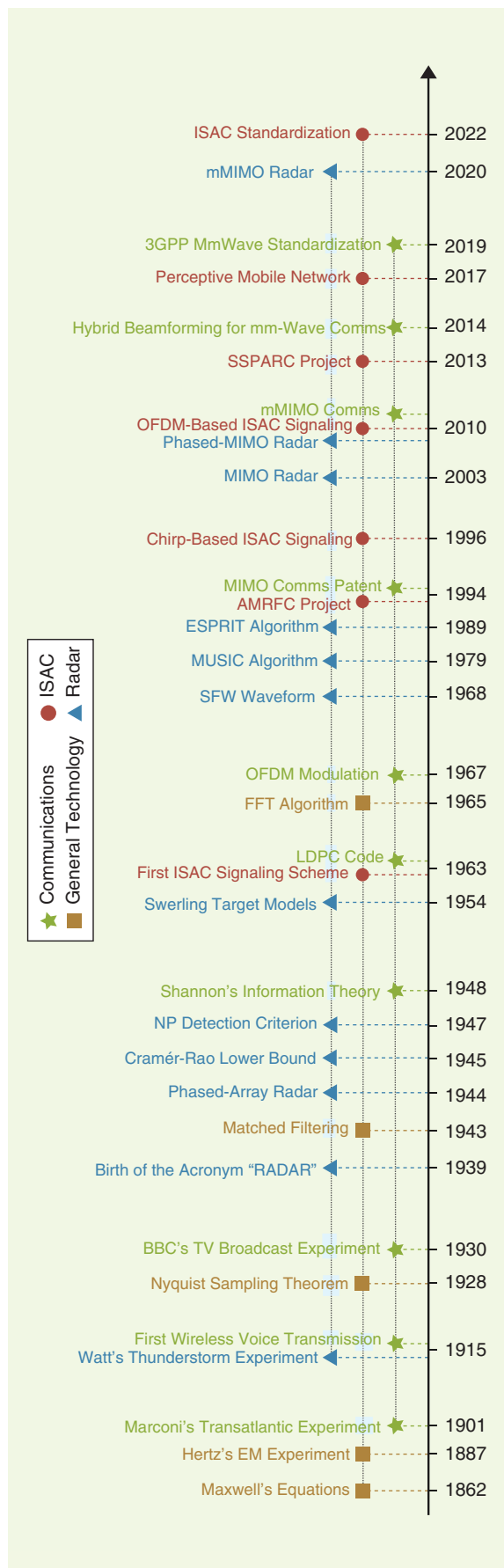


FIGURE 1. The important milestones for R&C SP: NP: Neyman-Pearson; LDPC: low-density parity check; FFT: fast Fourier transform; OFDM: orthogonal frequency-division multiplexing; SFW: stepped frequency waveform; AMRFC: Advanced Multifunction Radio Frequency Concept; MIMO: multiple-input, multiple-output; mMIMO: massive MIMO; 3GPP: 3rd Generation Partnership Project.

from single-antenna systems to phased arrays and from multiple-input, multiple-output (MIMO) to massive MIMO (mMIMO) and distributed antenna systems. Following the two technological trends, the paths of R&C eventually move from separation to integration and give rise to the ISAC technology, which motivates the detailed discussion on the SP framework of ISAC. Finally, we summarize the article and identify future research directions.

Fundamentals of radar and communications

Basic principles: A signals and systems perspective

The basic system setting for both R&C consists of three parts: a transmitter (Tx), which produces EM waves; a channel, over which EM waves propagate; and a receiver (Rx), which receives EM waves distorted by the channel. While communication Txs and Rxs are usually well separated, radar Txs and Rxs may be either colocated or separately positioned, leading to monostatic and bistatic radar settings, respectively. In more complicated scenarios, multiple Txs and Rxs may be involved in both applications, which correspond to multiuser communications and multistatic radar systems.

It is often convenient to represent EM waves by the electrical field intensity as a complex signal as a function of time t . The core tasks for R&C can then be defined as

- **Information acquisition for radar:** The aim here is to extract target information embedded in the received signal, given knowledge of the transmit signal.
- **Information delivery for communications:** The aim here is to recover useful information contained in the transmit signal at the communication Rx, with knowledge of the channel response.

By denoting the signals at the Tx and Rx at time t as $s(t)$ and $y(t)$, respectively, the propagation of the signal within the channel can be modeled as a mapping from its input $s(t)$ to the output $y(t)$. Ideally, if the noise and disturbance are not considered, such a mapping is linear due to the physical nature of EM fields and waves and, equivalently, owing to the linearity of Maxwell's equations. Furthermore, if the channel characteristics remain unchanged within a certain time period, the mapping can be approximated as a linear time-invariant system characterized by its impulse response $h(t)$. Thus, the linear mapping is expressed as a convolution integral $y(t) = (s * h)(t)$. While the signaling pulses may be of different forms for R&C, we suppose that a Nyquist pulse is leveraged such that $s(t)$ is substantially time limited on a finite interval $[-T, T]$. Therefore, a signal can be sampled in a nearly lossless manner after passing through the pulse shaping filter at the Rx, expressed as a convolution sum $y(n) = (s * h)(n)$ at the n th sampling point. Let $\mathbf{s} = [s(-N), \dots, s(N)]^T$ be the Tx signal, with length $2N + 1$; $\mathbf{h} = [h(0), \dots, h(P - 1)]^T$ be the channel impulse response, with length P ; and $\mathbf{y} = [y(-N), \dots, y(N + P - 1)]^T$ be the Rx signal, with length $2N + P$. Then, the convolution can be recast as $\mathbf{y} = \mathbf{H}\mathbf{s}$, where

$\mathbf{H} = \text{Toep}(\mathbf{h}) \in \mathbb{C}^{(2N+P) \times (2N+1)}$ is a Toeplitz matrix, with the n th column being $[\mathbf{0}_{n-1}^T, \mathbf{h}^T, \mathbf{0}_{2N-n+1}^T]^T$. Alternatively, one may express \mathbf{y} as $\mathbf{y} = \mathbf{S}\mathbf{h}$ by the commutative property of the convolution sum, where $\mathbf{S} = \text{Toep}(\mathbf{s}) \in \mathbb{C}^{(2N+P) \times P}$.

R&C have been largely treated as two separate research fields, due to different constraints in their respective applications, and were therefore independently investigated and developed.

The preceding duality between interchangeable signals and systems implies an interesting connection between R&C. From the communication perspective, the process of the Tx signal passing through a channel may be viewed as a linear transform \mathbf{H} applied to \mathbf{s} , with the communication task being to recover the information embedded in \mathbf{s} by receiving \mathbf{y} . From the radar perspective, the sensing task is to recover the target parameters embedded in \mathbf{h} , which is viewed as an input "signal," by observing \mathbf{y} , which

is viewed as an output signal linearly transformed from \mathbf{h} through a "system" \mathbf{S} . This reveals that the basic SP problems in R&C are mathematically similar.

Linear Gaussian models

Consider the more general linear Gaussian signal model by taking additive white Gaussian noise into account:

$$\mathbf{Y} = \mathbf{H}(\boldsymbol{\eta})\mathbf{S}(\boldsymbol{\xi}) + \mathbf{Z} \quad (1)$$

where \mathbf{Y} and \mathbf{S} are the sampled receive and transmit signals, which could be defined over multiple domains, e.g., the time–space and time–frequency domains; \mathbf{H} is the corresponding channel matrix (not necessarily Toeplitz); and \mathbf{Z} is the white Gaussian noise signal, with variance σ^2 . The channel \mathbf{H} is a function of the physical parameters $\boldsymbol{\eta}$, e.g., range, angle, and Doppler. The transmit signal \mathbf{S} may be encoded/modulated with some information codewords $\boldsymbol{\xi}$. Model (1) represents many R&C systems, as elaborated in the following:

- **Radar signal model:** Radar systems aim at extracting target parameters $\boldsymbol{\eta}$ from \mathbf{Y} . For both radar Txs and Rxs, \mathbf{S} is typically a known deterministic signal, in which case $\boldsymbol{\xi}$ can be omitted since the radar waveform contains no information. This can be expressed as

$$\mathbf{Y}_r = \mathbf{H}_r(\boldsymbol{\eta})\mathbf{S}_r + \mathbf{Z}_r. \quad (2)$$

- **Communication signal model:** Communication systems aim at recovering codewords $\boldsymbol{\xi}$ from \mathbf{Y} . The channel \mathbf{H} , which is sometimes regarded as an unstructured matrix, can be estimated a priori via pilots. Therefore, knowing $\boldsymbol{\eta}$ may not be the first priority. The resulting model is

$$\mathbf{Y}_c = \mathbf{H}_c\mathbf{S}_c(\boldsymbol{\xi}) + \mathbf{Z}_c. \quad (3)$$

The subscripts $(\cdot)_r$ and $(\cdot)_c$ are to differentiate R&C signals, channels, and noises, respectively. We highlight that (2) and (3) describe a variety of R&C signal models. For example, (2) can be viewed as the target return of a MIMO radar in a given range-Doppler bin, where $\boldsymbol{\eta}$ represents angles of targets.

Similarly, (3) may be considered a narrowband MIMO communication signal. Alternatively, both (2) and (3) can be viewed as orthogonal frequency-division multiplexing (OFDM) signal models for R&C, respectively. In the following, we do not specify the signal domain but focus on generic models (2) and (3). More concrete signal models are discussed in the “Spectrum Engineering: The Road to Higher Frequency and Larger Bandwidth” and “Scaling Up the Antenna Array: The Road From Single Antenna to mMIMO” sections. In addition to individual R&C systems, (1) may also characterize the general ISAC signal model. That is, a unified ISAC signal serves dual purposes of information delivery and target sensing, whereas R&C channels may differ from one another. More details on ISAC systems will be discussed in the “ISAC: The Road From Separation to Integration” section.

Fundamental signal processing theories

In the following, we elaborate on the fundamental SP theories of R&C and, in particular, focus on (2) and (3).

Signal detection

Signal detection problems arise from many R&C applications. One essential task for radar is to determine whether a target exists by observing \mathbf{Y}_r , modeled as a binary hypothesis testing (BHT) problem:

$$\mathbf{Y}_r = \begin{cases} \mathcal{H}_0: \mathbf{Y}_r = \mathbf{Z}_r \\ \mathcal{H}_1: \mathbf{Y}_r = \mathbf{H}_r(\boldsymbol{\eta})\mathbf{S}_r + \mathbf{Z}_r \end{cases} \quad (4)$$

where \mathcal{H}_0 represents the null hypothesis, i.e., the radar receives nothing but noise, and \mathcal{H}_1 stands for the hypothesis where the radar receives both the target return and noise. To address the preceding BHT problem, one may need to design a detector $\mathcal{T}(\cdot)$ that maps the received signal \mathbf{Y}_r to a real number and then compare the output with a preset threshold γ to determine which hypothesis to choose as true. A target detector may, for example, maximize the detection probability $P_D = \Pr(\mathcal{H}_1 | \mathcal{H}_1)$ while maintaining a low false alarm probability $P_{FA} = \Pr(\mathcal{H}_1 | \mathcal{H}_0)$, following the Neyman–Pearson (NP) criterion [7].

Signal detection also plays a critical role at the communication Rx. In (3), the communication Rx observes $\mathbf{Y}_c = \mathbf{H}_c\mathbf{S}_c(\boldsymbol{\xi}) + \mathbf{Z}_c$ and seeks to yield an estimate $\hat{\boldsymbol{\xi}}$ of the information symbol vector $\boldsymbol{\xi} = [\xi_1, \xi_2, \dots, \xi_N]^T \in \mathcal{A}$. This problem can be solved by leveraging the minimum error probability (MEP) criterion, that is, to minimize the error probability $P_e = \sum_{i=1}^{|\mathcal{A}|} \Pr(\hat{\xi}_i \neq \xi_i) \Pr(\xi_i)$, where $|\mathcal{A}|$ is the cardinality of \mathcal{A} . The MEP criterion can be translated to the maximum a posteriori criterion; i.e., the recovered symbols should be the maximizer of the a posteriori probability. Note that the decision region in the MEP criterion for communication symbols is determined by their a priori probability, while the decision thresholds in the NP criterion for radar are determined by the required false alarm probability, resulting in different designs for R&C detectors.

The boundary between R&C is becoming blurred, and hardware and spectrum convergence has led to a design paradigm shift, where the two systems can be codesigned.

Parameter estimation

Parameter estimation represents another category of basic SP techniques in R&C systems. For a radar system, once a target is confirmed to be present, the system needs to further extract the target’s parameters $\boldsymbol{\eta}$ from \mathbf{Y}_r by conceiving an estimator mapping \mathbf{Y}_r from the signal space to an estimate $\hat{\boldsymbol{\eta}}$, defined as $\hat{\boldsymbol{\eta}} = \mathcal{F}(\mathbf{Y}_r)$. To measure how accurate an estimator is, a possible performance metric is the mean square error (MSE), expressed as $\varepsilon = \mathbb{E}(\|\boldsymbol{\eta} - \hat{\boldsymbol{\eta}}\|^2)$. The average may be over the noise and also over the parameters if they are assumed to be random. When the parameters are assumed to be deterministic, the MSE of any unbiased estimate is lower bounded by the Cramér–Rao bound (CRB), defined as the inverse of the Fisher information matrix \mathbf{J} [7]:

$$\mathbb{E}[(\boldsymbol{\eta} - \hat{\boldsymbol{\eta}})(\boldsymbol{\eta} - \hat{\boldsymbol{\eta}})^H] \succeq \mathbf{J}^{-1} = \left\{ -\mathbb{E} \left[\frac{\partial^2 \ln p(\mathbf{Y}_r; \boldsymbol{\eta})}{\partial \boldsymbol{\eta}^2} \right] \right\}^{-1} \quad (5)$$

where $p(\mathbf{Y}_r; \boldsymbol{\eta})$ is the probability density function of \mathbf{Y}_r parameterized by $\boldsymbol{\eta}$. While the maximum likelihood estimate (MLE) asymptotically achieves the CRB, attaining the MLE can be highly computationally expensive. To that end, low-complexity parameter estimation algorithms, e.g., MUSIC and ESPRIT [8], [9], have been widely applied in practical situations, such as angle-of-arrival estimation.

In communication systems, the channel \mathbf{H}_c should be estimated before delivering the useful information. For channel estimation, the Tx sends pilots to the Rx, which are reference signals known to both. The Rx then estimates the channel based on both the received signals and pilots. Channel estimation is mathematically similar to the target estimation problem, where the to-be-estimated parameters $\boldsymbol{\eta}$ are entries of \mathbf{H}_c , which is regarded as an unstructured matrix. We elaborate on similarities and differences among estimation tasks for communication channels and radar targets in the “Scaling Up the Antenna Array: The Road From Single Antenna to Massive MIMO” section.

Information theory

Information theory serves as the foundation of communication SP. A remarkable result attained by Shannon in his landmark paper [10], published in 1948, states that, for any discrete memoryless channel with input X and output Y , the channel capacity is $C = \max_{p(X)} I(X; Y)$, where the maximum is taken over all possible input distributions $p(X)$, and $I(X; Y)$ is the mutual information (MI) between X and Y . The channel coding theorem states that a coding rate R below C is achievable. Conversely, if $R > C$, an arbitrarily small decoding error is not possible. Information theory may also be adopted to measure radar performance [11] and may reveal profound connections between R&C. Let us consider a generic real-valued Gaussian channel with an input X , which is assumed to be random, and output Y . In the communication case, X can be an information-carrying signal emitted by the Tx, and Y can be the signal received at the

communication Rx. In the radar case, X can be some random target parameter/channel to be estimated, and Y can be the echo signal received at the radar Rx. In both R&C tasks, we may wish to accurately/approximately recover X by observing Y .

We denote the MI between X and Y as $I(X; Y)$ and the minimum MSE (MMSE) of estimating X from Y as $\text{MMSE}(X|Y) = \mathbb{E}\{|X - \mathbb{E}(X|Y)|^2\}$, both of which may be expressed as functions of the signal-to-noise ratio (SNR), namely, $I(\text{snr})$ and $\text{MMSE}(\text{snr})$. We then have the following I -MMSE identity, which holds for Gaussian channels [12]:

$$\frac{d}{d\text{snr}} I(\text{snr}) = \frac{1}{2} \text{MMSE}(\text{snr}). \quad (6)$$

The preceding relationship implies that the increasing rate (derivative) of the MI between X and Y with respect to the SNR is half of the MMSE for estimating X given Y . For a Gaussian channel, $I(\text{snr})$ is maximized by inputting a Gaussian distributed X under a given SNR. More precisely, a Gaussian input always results in the most rapidly growing MI and, accordingly, yields the maximum MMSE, making it the most favorable for communication yet the least favorable for radar sensing. From a communication perspective, the channel input should be “as random as possible” to carry more information. From a radar perspective, estimation performance becomes more inaccurate if the target parameters change more randomly. The Gaussian distribution has the highest entropy (randomness) under a second-order moment constraint (i.e., a fixed power budget), resulting in this interesting tradeoff.

Interplay between radar and communications

While communication happens between cooperative Tx and Rx, radar sensing is essentially uncooperative, even if the radar Tx and Rx are colocated. This distinction results in inherently different R&C SP frameworks. First, R&C SP aims at recovering useful information contained in the received signal, with minimum distortion. The communication system, however, needs another level of performance guarantee, i.e., to transmit, receive, and actively control as much information as possible. This requires sophisticatedly tailored encoding and decoding and modulation and demodulation strategies at the Tx and Rx, respectively, which motivates the development of information theory, whose spirit forms the foundation of the modern communication SP framework. Moreover, as the communication Tx and Rx are highly cooperative, they are able to share the SP complexities in a rather flexible manner, depending on the specific scenarios. For instance, in a downlink communication setup where a powerful base station (BS) sends information to the user, most of the complicated SP is done at the Tx’s side, e.g., precoding, to ease the computational burden at the user’s side. In a radar system, however, the complexity of the Rx SP always dominates its Tx counterpart, yet they are typically unable to share design complexities.

In what follows, we elaborate on the evolution of R&C in terms of both spectrum engineering and antenna array technologies and further reveal their interplay in spectral and spatial SP.

Spectrum engineering: The road to higher frequency and larger bandwidth

Spectrum characteristics and management

The radio frequency (RF) EM spectrum, extending from below 1 MHz to above 100 GHz, has been used for a wide range of applications, including communications, radio and television broadcasting, radio navigation, and sensing [13]. Figure 2 displays the frequency bands where R&C systems operate and highlights the modes and usage that are performed in each band. For radar sensing, the lower bands offer some unique capabilities, such as long-range surveillance and weather monitoring [13]. For communications, lower bands exhibit low signal attenuation, making them suitable for long-distance transmission.

The higher-frequency bands provide some advantages to R&C. For a fixed fractional bandwidth, increasing the operating frequency subsequently increases the achievable bandwidth, thus providing finer range resolution for radar and higher data rates for communications. However, in these higher bands, long-range operation becomes more strongly affected by attenuation due to the atmosphere. Moreover, the diffraction effect of high-frequency EM wave signals decreases, which leads to a reduction in the number of paths propagated. Thus, radar sensing and wireless communication via these bands are limited to short-range applications. For example, radars from X to W-bands are used for automotive collision avoidance, police radar, airport surveillance, and scientific remote sensing. As for communication, the mm-wave band is soon to be finalized as part of the 5G New Radio standards and has been exploited by the 802.11ad/ay wireless local area network (WLAN) protocols. More advanced radar SP tasks, such as real-time range-Doppler imaging and target recognition, typically rely on sparse recovery methods, as sparse channels are usually required in radar applications. For communication with high frequency and wideband, algorithms are required to be specifically conceived for channel estimation and demodulation to achieve higher data rates.

As a representative wideband signaling strategy, multicarrier technologies have been extensively applied in both R&C systems, which we overview in the following.

Signal models and processing techniques

Multicarrier radar signal processing

Let us consider a pulsed radar with a nonzero support $[0, \tau]$ for each pulse. The radar works by transmitting a short burst of energy, or pulse, toward the target and then listening for the echo that bounces back. The pulse repetition interval (PRI) is T_{PRI} , and the total transmit bandwidth available at the baseband is B_r , resulting in a duty cycle of τ/T_{PRI} . The carrier frequency f_n of the n th pulse is chosen from $[f_c - \Delta B/2, f_c + B_r - \Delta B/2]$ for the multicarrier radar system, where f_c is the lowest carrier frequency within the band and ΔB is the bandwidth of each subpulse. Specifically, for single-carrier systems, we have $f_n = f_c$ for all n with $f_c \gg B_r$. The n th transmit pulse is

$$s_{r,n}(t) = \sqrt{P_r} x_r(t - nT_{\text{PRI}}) e^{j2\pi f_n(t - nT_{\text{PRI}})} \quad (7)$$

where P_r is the radar transmit power. For the linear frequency-modulated (LFM) waveform, we have $x_r(t) = e^{j\pi B_r t^2/\tau} \text{rect}(t/\tau)$, where $\text{rect}(t/\tau)$ is one for $0 \leq t \leq \tau$ and zero elsewhere. The target response is

$$h(t) = \sum_{l=0}^{L-1} \alpha_l e^{j2\pi\nu_l t} \bar{\delta}(t - \tau_l) \quad (8)$$

where $\bar{\delta}(\cdot)$ is the Dirac delta function, α_l is the reflection coefficient, and τ_l and ν_l are the delay and Doppler of the l th target, corresponding to its range and velocity. The time delay between the transmitted and received signals is used to calculate the distance to the target. In general, the radar cannot separate the two targets in range if $|\tau_{l_1} - \tau_{l_2}| < 1/B_r$. In many sensing problems, obtaining information at high range resolution is crucial to distinguish closely spaced targets [14], which incurs larger bandwidth needs.

In 1968, Ruttenburg and Ghanzi proposed the stepped frequency waveform (SFW), which can be viewed as a form of interpulse phase coding [15]. It transmits a series of linearly increasing or decreasing frequency signals, or steps, toward the target. The frequency of the received signal is compared to the frequency of the transmitted signal to calculate the distance to the target. By sweeping through a range of frequencies, the radar can also measure the target's speed. The SFW was later used in sets of radars, in which coherent integration of a burst of pulses yields high range resolution. Conventional SFW sets the carrier frequency sequence as $f_n = f_c + n\Delta f$ for all n . To improve the data rate and avoid interference, more recent approaches randomly draw frequencies from the set $\mathcal{F} = \{f_n | f_n = f_c + d_n\Delta f\}$, where Δf is a step size and $d_n \in \mathbb{Z}$ is chosen from a subset of $[0, D]$ so that $D\Delta f > B$ is the synthesized bandwidth.

Conventional SFW SP follows the matched filtering (MF) process, in which \mathbf{Y}_r , \mathbf{S}_r , and $\mathbf{H}_r(\boldsymbol{\eta})$ are the Rx signal, Tx signal, and target response in the frequency domain, respectively. With this, we may represent the discretized signal as $\mathbf{y} = \mathbf{S}\mathbf{h} + \mathbf{z}$, with \mathbf{h} being the time-domain target response and \mathbf{S} being the Toeplitz matrix composed of the transmitted signal. For sparse SFW, MF may lead to high sidelobes due to the vacancy in frequency bands. To mitigate the effects of sidelobes, radar designers can use a variety of techniques, such as antenna designs that minimize sidelobes, SP algorithms that filter out sidelobes, and adjusting the radar's operating parameters to avoid sidelobe interference. More recent approaches consider the sparse nature of radar signals and estimate the target parameters by using sparse recovery algorithms. Assuming that the targets are composed of very few scatterers compared with the number of measurements, \mathbf{h} can be estimated by solving the optimization problem

$$\min_{\mathbf{h}} \|\mathbf{h}\|_0 \text{ s.t. } \|\mathbf{y} - \mathbf{S}\mathbf{h}\|_2 \leq \zeta \quad (9)$$

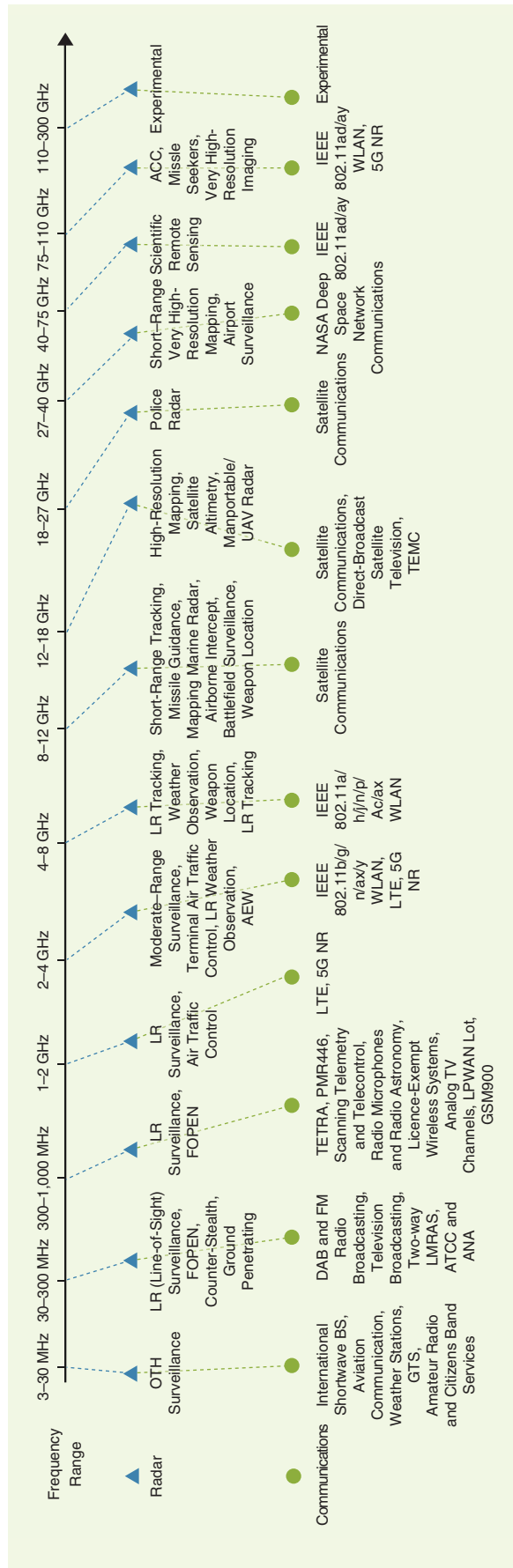


FIGURE 2. A summary of frequency bands and their usage in R&C applications. AEW: airborne early warning; ACC: automobile cruise control; UAV: unmanned aerial vehicle; LR: long range; FOPEN: foliage penetration; GPR: ground penetrating radar; OTH: over the horizon; ATCC: air traffic control communications; LMRAS: land mobile radio system; TETRA: terrestrial trunked radio; TEMC: terrestrial microwave communications; GTS: government time station; ANA: air navigation; DAB: digital audio broadcasting; FM: frequency modulation; PMR: private mobile radio; LPWAN: low-power wide area network; loT: Internet of Things; NR: New Radio; WLAN: wireless local area network.

where ζ is a positive constant dependent on the noise variance. This problem can be solved using compressed sensing algorithms, e.g., ℓ_1 -norm minimization, and greedy algorithms, such as orthogonal matching pursuit [16], [17].

Multicarrier communication SP

As for the communication system, we assume it occupies a frequency band of B_c . Setting $T_c = 1/B_c$, the radiated signal is given by

$$s_c(t) = \sum_{n=0}^{N_s-1} \sqrt{P_c} x_c(n) \psi_c(t - nT_c) e^{j2\pi f_c t} \quad (10)$$

where P_c is the transmit power, $x_c(n)$ for all n is the symbol sequence to be transmitted with length N_s , and $\psi_c(\cdot)$ satisfies the Nyquist criterion with respect to T_c . Classic amplitude shift keying (ASK), frequency shift keying (FSK), and phase shift keying (PSK) could be applied for generating $x_c(n)$.

The model in (10) is a single-carrier system, which has limitations in bandwidth and data rates. Following a 1965 article, Zimmerman and Kirsch designed a high-frequency radio multicarrier transceiver [18]. When the structure in signal space relies on multiple subcarriers, it corresponds to a multicarrier scheme represented by letting $x_c(n) = \sum_{m=0}^{N_c-1} x_{c,m}(n) \psi_{c,m}(t - nT_c)$. Here $x_{c,m}(n)$ is the symbol sequence being transmitted, N_c is the number of subcarriers, and $\psi_{c,m}(t)$ is the synthesis function that satisfies the Nyquist criterion with respect to $1/B_c$ and maps $x_{c,m}(n)$ into the signal space. The family of $\psi_{c,m}(t) = \omega_c(t) e^{j2\pi m \Delta f t}$ is referred to as a *Gabor system*, where $\omega_c(t)$ is the prototype filter and Δf is the subcarrier spacing. It is easy to show that an N_c -point inverse discrete Fourier transform operating on the data generates samples of the OFDM signal, which can be accelerated by the fast Fourier transform (FFT) algorithm proposed by Cooley et al. [19]. At the communication Rx, we remove the cyclic prefix and take the signal samples for $n = 0, 1, \dots, N_s - 1$, yielding

$$\mathbf{S} = \mathbf{F}_{N_c}^H (\mathbf{X}_c \odot \mathbf{b}(\tau') \mathbf{c}(\nu)^T) \quad (11)$$

where \mathbf{F}_N is an N -dimensional discrete Fourier transform matrix; \odot is the Hadamard product; $\mathbf{X}_c = [\mathbf{x}_c(0), \mathbf{x}_c(1), \dots, \mathbf{x}_c(N_s - 1)]$, with $\mathbf{x}_c(n) = [x_{c,0}(n), x_{c,1}(n), \dots, x_{c,N_c-1}(n)]^T$; $\mathbf{b}(\tau') = [1, e^{-j2\pi \Delta f \tau'}, \dots, e^{-j2\pi (N_c-1) \Delta f \tau'}]^T$, with τ' being the time delay; and $\mathbf{c}(\nu) = [1, e^{-j2\pi f_c T_c \nu}, \dots, e^{-j2\pi f_c (N_s-1) T_c \nu}]^T$, with $f_c \nu$ being the Doppler shift. Then, the FFT could be applied before the detection of symbols $x_{c,m}(n)$ for $m = 0, 1, \dots, N_c - 1$.

In most practical scenarios, the radio channel is both time and frequency dispersive such that the channel output spreads over time and frequency domains. Such channel distortion results in so-called intersymbol interference (ISI) and interchannel interference (ICI) onto the received signals. By defining the time–frequency lattice based on symbol duration and subcarrier bandwidth, namely, the time–frequency plane, ISI and ICI can be reduced via well-localized 2D pulse shaping filters. Unfortunately, simultaneously sharply localizing a time- and frequency-limited signal on the time–frequency

plane to well concentrate its energy is impossible, as stated by the Heisenberg uncertainty principle.

Interplay between radar and communications

Pulse shaping for radar and communications

Pulse shaping is essential for both R&C to shape the waveform of the transmitted signal. Although signaling pulses serve a similar purpose in both cases, there are some key differences in their design and implementation. In communication systems, pulse shaping is used primarily to minimize ISI and control the bandwidth of the transmitted signal. This helps optimize the data rate, signal quality, and spectral efficiency. In radar systems, in addition to bandwidth control, pulse shaping is applied to control the sidelobes of the transmitted waveform. This helps to improve the range resolution and target detection capability. Furthermore, in communication systems, common pulse shaping filters include the raised cosine filter, root raised cosine filter, Gaussian filter, and various others. These filters are chosen based on the specific modulation scheme, channel conditions, and system requirements. In radar systems, common pulse shaping filters include the Hamming window, Blackman window, Chebyshev window, and Taylor window, among others. These filters are chosen based on the radar's specific requirements, such as the desired peak sidelobe level and range resolution.

OFDM-based radar versus delay-Doppler communications

Multicarrier techniques have been extensively used over the past decade for wideband systems. Examples include the SFW for radars and OFDM for communications. It is worth noting that the OFDM signal can also be used for radar sensing, which is known as the *communication-centric ISAC waveform*, which is elaborated later. In such a system, the ISAC Tx transmits signals jointly for radar sensing and communicating with other communication systems by using the same OFDM signal, where each symbol is individually modulated with data belonging to a constellation. Accordingly, the OFDM blocks are individually processed at the Rx of the ISAC system. While the communication processing consists of extracting modulated data from each block, the radar processing consists of estimating the range-Doppler profile through the 2D FFT operation [20]. As discussed in the previous section, ISI and ICI cannot be fully eliminated in OFDM systems. To ease such issues, the recently developed orthogonal time–frequency space (OTFS) modulation proposed to use the delay-Doppler (DD)-based signal representation to convert the time–frequency channel responses into simple 2D time-invariant channel response [21], thus alleviating the time–frequency selective effects. In such a case, the available signal propagation paths become physically explainable, observable, and probably predictable by, for example, moving object tracking strategies [22]. These key observations mandate that the OTFS be a novel ISAC SP paradigm that goes beyond separately performing R&C SP on the DD and time–frequency domains.

Scaling up the antenna array: The road from single antenna to massive MIMO

In the past decade, the evolution of R&C systems has gained considerable spatial efficiency by scaling up antenna arrays. The more antennas equipped at the Tx/Rx, the more degrees of freedom (DoFs) signaling strategies can exploit from the propagation channel, and better reliability can be achieved in the transmission. In this section, we investigate the evolution path of the array structure.

Array structure evolution and signal models

In general, an antenna array can be described by its response (also known as a steering vector), which is a vector function of angle parameters θ , denoted as $\mathbf{a}(\theta)$. For an N -antenna uniform linear array with antenna spacing d and wavelength λ , the steering vector is expressed as

$$\mathbf{a}(\theta) = \left[1, e^{-j2\pi\frac{d}{\lambda}\sin(\theta)}, e^{-j4\pi\frac{d}{\lambda}\sin(\theta)}, \dots, e^{-j(N-1)\pi\frac{d}{\lambda}\sin(\theta)} \right] \quad (12)$$

where $\theta \in [-\pi, \pi]$ and d is typically set as $\lambda/2$. Suppose that the radar or communication system is equipped with N_t and N_r antennas at its Tx and Rx and that the signal arrives from L resolvable paths. The general channel matrix for both R&C can be modeled as

$$\mathbf{H} = \sum_{l=1}^L \alpha_l \mathbf{b}(\theta_l) \mathbf{a}^T(\phi_l) \quad (13)$$

where α_l , ϕ_l , and θ_l are the channel coefficient, direction of departure, and direction of arrival (DOA) for the l th signal path; $\mathbf{a}(\phi) \in \mathbb{C}^{N_t \times 1}$ and $\mathbf{b}(\theta) \in \mathbb{C}^{N_r \times 1}$ are Tx and Rx steering vectors, respectively. The channel model (13) may represent L resolvable point targets for radar or L propagation paths for communication. In the communication case, α_l is contributed by both the path loss and small-scale fading effect. In the radar case, α_l may also be contributed by the radar cross section (RCS) of the targets in addition to the round-trip path loss, which follows Swerling's target models [23].

Phased array

Having the capability of generating a highly directive beam through rapid electronic phase control, phased-array techniques triggered various R&C innovations. The phased-array

system, in its simplest form, consists of a single RF chain connected with multiple antennas through phase shifters (Figure 3). In other words, the signal transmitted over each antenna is a phase-shifted counterpart of the signal generated in the RF chain. If both the Tx and Rx are equipped with phased arrays, the discrete receive signal at time instant n can be expressed as

$$y_n = \mathbf{w}^H \mathbf{H} \mathbf{f} s_n + z_n, \forall n \quad (14)$$

where s_n is the signal transmitted within the Tx's RF chain and $\mathbf{f} \in \mathbb{C}^{N_t \times 1}$ and $\mathbf{w} \in \mathbb{C}^{N_r \times 1}$ consist of the phase shifters at the Tx and Rx, with each of their entries being constant modulus, which are also known as the *transmit beamformer* and *receive combiner*, respectively, and are referred to as *RF/analog beamforming*.

MIMO (digital) array

In contrast to the phased array, the MIMO system is equipped with multiple RF chains, where each RF chain is connected to a single antenna port. The receive signal for a MIMO system can be modeled as

$$\mathbf{y}_n = \mathbf{H} \mathbf{F} \mathbf{s}_n + \mathbf{z}_n, \forall n \quad (15)$$

where $\mathbf{s}_n \in \mathbb{C}^{K \times 1}$ and $\mathbf{y}_n \in \mathbb{C}^{N_r \times 1}$ are transmit and receive signal vectors at the Tx and Rx, respectively, with K being the number of independent signals and $\mathbf{F} \in \mathbb{C}^{N_t \times K}$ a digital precoder. In MIMO radar applications, $\mathbf{s}_n, \forall n$ are spatially orthogonal waveforms, and \mathbf{F} may be designed to steer the signals to multiple directions simultaneously and to keep the orthogonality for omnidirectional searching. In MIMO communication applications, \mathbf{F} may be designed to equalize and exploit the multipath effect by using various precoding techniques, e.g., zero forcing and MF precoding. MIMO communication technology was first patented in 1994 [24], which inspired the invention of the MIMO radar concept, in 2003 [25].

mMIMO array

When the antenna number grows extremely large, e.g., above 100, the MIMO system becomes an mMIMO system, or a large-scale antenna system. In this case, the steering vectors are

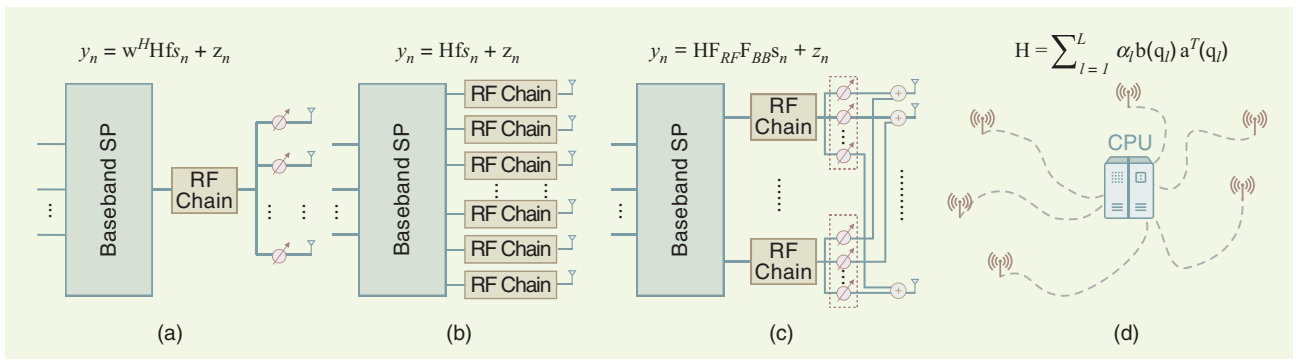


FIGURE 3. The antenna array evolution and signal models: the (a) phased array, (b) MIMO/mMIMO array, (c) hybrid array, and (d) distributed array.

asymptotically orthogonal to one another. Moreover, in a richly scattering environment with a large L , for $N_t \rightarrow \infty, N_t \gg N_r$, we have $\text{var}(\|\mathbf{h}_k\|^2)/\mathbb{E}(\|\mathbf{h}_k\|^2) \rightarrow 0, \forall i$ and $(1/N_t)\mathbf{H}\mathbf{H}^H \approx \mathbf{I}_{N_r}$, which are known as the *channel hardening effect* and *favorable propagation effect*. While the basic signal model for mMIMO remains the same as (15), it has additional superiorities over small-scale MIMO [4]. First, one may attain even more DoFs if equipping both the Tx and Rx with mMIMO arrays. More importantly, the channel hardening effect improves the communication reliability by generating a nearly deterministic channel, which considerably simplifies the SP. Recent research has also shown the superiority of applying the mMIMO technology to the radar system, which is able to detect a target via a single snapshot in the presence of a disturbance with unknown statistics [26].

Hybrid array

Massive MIMO achieves dramatic gains at the price of a growing number of antennas and RF chains, incurring larger hardware costs. To that end, the hybrid analog–digital array was proposed as a promising solution [27]. The hybrid array can be viewed as a tradeoff between the phased-array and fully digital MIMO array, as it connects fewer RF chains with massive antennas through phase shifters and switches. Consider a hybrid array with N_{RF} RF chains and N_t antennas. The phase shifter-based design has the following signal model:

$$\mathbf{y}_n = \mathbf{H}\mathbf{F}_{\text{RF}}\mathbf{F}_{\text{BB}}\mathbf{s}_n + \mathbf{z}_n, \forall n \quad (16)$$

where $\mathbf{F}_{\text{RF}} \in \mathbb{C}^{N_t \times N_{\text{RF}}}$ is the analog beamforming matrix containing constant-modulus entries representing phase shifters and $\mathbf{F}_{\text{BB}} \in \mathbb{C}^{N_{\text{RF}} \times K}$ is a digital precoder multiplexing K data streams. The hybrid array is also known as the *phased-MIMO structure* in the radar community [28]. In addition to reducing the cost for implementing MIMO radar, it achieves a balance between phased-array and MIMO radars via harvesting performance gains from both. By partitioning the antenna array into different subarrays, phased-MIMO radar may formulate highly directional beams toward targets at each subarray, improving the SNR of the echoes. In the meantime, it may also transmit orthogonal waveforms over different subarrays, thus reaping the gain of waveform diversity.

Distributed array

The continually growing demands for connectivity, coverage, and high-resolution sensing necessitate research of the distributed antenna array system for both R&C. Instead of colocating the antennas in a compact space, distributed antennas are spread over a large area while connecting to a central processing unit (CPU), providing a much higher probability of coverage and an improved diversity gain. Distributed antenna systems have been extensively studied from the communication viewpoint under different names, including networked MIMO, coordinated multipoint and cell-free mMIMO [29]. Their radar counterparts, on the other hand, are known as *multistatic radar* and *MIMO radar with widely separated antennas* [30]. The distributed array may

also be described by its response, which, however, is no longer a function of the angle; rather, it is a function of the coordinates of the targets and scatterers in each signal path. By denoting the coordinates of the l th target/scatterer as $\mathbf{q}_l = (x_l, y_l)$, the distributed channel matrix can be expressed as

$$\mathbf{H} = \sum_{l=1}^L \alpha_l \mathbf{b}(\mathbf{q}_l) \mathbf{a}^T(\mathbf{q}_l). \quad (17)$$

Note that the specific array geometry relies upon the overall deployment of the distributed system.

Signal processing for MIMO radar and communications

Colocated MIMO radar

With colocated antennas, MIMO radars can mimic beamformers utilizing low-probability-of-intercept waveforms. Rather than focusing energy on a target, the transmitted energy is evenly distributed in space [3], [30]. Compared to conventional phased-array beamforming, the loss of processing gain due to the uniform illumination is compensated by the gain in time since there is no need to scan a narrow beam [3], [30]. The beamforming of classic colocated MIMO computes the correlations between the observation vectors from the previous step and the steering vectors corresponding to each azimuth/elevation on the grid defined by the array aperture. Then, the targets can be detected in the angular domain. It is worth noting that a heuristic detection process, in which there is knowledge of the number of targets, clutter location, and so on, may help in discovering targets' positions [31]. For example, if we know there are M targets, then we can choose the M strongest points in the targets profile. Alternatively, constant false alarm rate detectors determine a power threshold, above which a peak is considered to originate from a target so that a required false alarm probability is achieved.

Distributed MIMO radar

Widely separated transmit/receive antennas capture the spatial diversity of the target's RCS [30]. Practical realization of phase coherency may be difficult, thus often necessitating noncoherent combining to perform target detection using the distributed apertures [30]. It is shown that with noncoherent processing, a target's RCS spatial variations can be exploited to obtain a diversity gain for target detection and for estimation of various parameters, such as the DOA and Doppler. Again, Swerling models [23] can be used to represent the statistical RCS fluctuations as a function of the target decorrelation time. In distributed MIMO radars, a multidimensional signal space is created when the returns from multiple scatterers and targets combine to generate a rich backscatter. By exploiting the spatial dimension, MIMO radar with widely separated antennas may overcome bandwidth limitations and support high-resolution target localization [30].

MIMO communications

MIMO communication has been playing a critical role in cellular and Wi-Fi systems since the 2010s, the beginning of the 4G era. Early SP methods focused on single-user MIMO (SU-MIMO)

communication, where a multiantenna BS serves a single or multiantenna user, which is also known as the *point-to-point MIMO channel*. In addition to multiplexing more data streams, the MIMO array is able to serve multiple users over the same time–frequency resource block, which is known as *multiuser MIMO (MU-MIMO)* communications technology. Compared to SU-MIMO, the MU-MIMO configuration offers significant complexity reduction at the users’ side. For MU-MIMO systems, the coordinated signal detection at the Rx’s side is not as straightforward as in SU-MIMO since cooperation among users is difficult. Therefore, the BS needs to precancel the interference by employing various precoding methods, which also simplifies the SP at the users’ side. While dirty paper coding is capacity achieving, it suffers from high complexity [32]. Therefore, suboptimal linear precoders are more commonly employed in practical systems.

Interplay between radar and communications

Multiplexing versus diversity

The expansion of the antenna array brings diversity and multiplexing gains, which are cornerstones of MIMO communication theory. Transmit or receive diversity is a means to combat deep fading by creating different propagation paths through the Tx–Rx antenna pairs. Multiplexing, on the other hand, exploits the DoFs provided by the multipath propagation environment through sending different data streams over independent subchannels. In 2003, Zheng and Tse revealed that there is an inherent tradeoff between the two gains, namely, the diversity–multiplexing tradeoff (DMT) [33]. For an independent identically distributed Rayleigh MIMO channel $\mathbf{H}_c \in \mathbb{C}^{N_r \times N_t}$, the maximum diversity gain and multiplexing gain are $N_t N_r$ and $\min\{N_t, N_r\}$, respectively. From a broader viewpoint, the DMT is essentially a tradeoff between reliability and efficiency.

The spirit of MIMO radar SP can be interpreted in a similar manner. On the one hand, colocated MIMO radar possesses the superior attribute of waveform diversity, which means that diverse waveforms are flexibly emitted through different antennas. Waveform diversity may be implemented in either the baseband or RF band, e.g., through phase coding or frequency coding. It significantly improves parameter identifiability compared to its phased-array counterpart. That is, the colocated MIMO radar is able to uniquely identify up to $\mathcal{O}(N_t N_r)$ targets, which is N_t times of that of phased-array radar [3]. This connects more closely to the multiplexing gain in communications. On the other hand, distributed MIMO radar provides target RCS diversity. By widely spreading the antennas, distributed MIMO radar is able to observe a target from different directions, thus providing stable sensing performance by overcoming the drastic RCS fluctuations in high-mobility targets [30].

The preceding discussion again reflects the signals and systems duality. Since the signals and systems are interchange-

able, we may view radar target channels as “signals” and radar waveforms as “systems.” While the basic model for MIMO communications is that multiple data streams (signals) are transmitted through multiple spatial channels (systems), the model for MIMO radar is, conversely, that multiple target channels (signals) pass through diverse waveforms (systems). This duality creates the interesting interplay between R&C, and may imply more essential connections and tradeoffs in ISAC systems.

Since the signals and systems are interchangeable, we may view radar target channels as “signals” and radar waveforms as “systems.”

Statistical versus geometrical channel representations

Most of the MIMO radar channels are geometrically modeled, as the ultimate goal of the radar is to extract the physical parameters of targets. The MIMO communication channel, on the other hand, can be modeled either statistically or geometrically, depending on the specific scenarios and systems. The distinct models of the same channel are representations in different coordinate systems. For instance, an $N_r \times N_t$ communication channel matrix \mathbf{H}_c may be generally seen as a point in the Euclidean space $\mathbb{C}^{N_r \times N_t}$. If it is geometrically modeled, then it may be viewed as a point in a subspace spanned by steering vectors $\mathbf{a}(\phi_l)$ and $\mathbf{b}(\theta_l)$. In sub-6-GHz bands with richly scattering environments, the small-scale MIMO channel is modeled as an unstructured matrix subject to certain distributions, e.g., Rayleigh and Rician distributions, since the number of propagation paths could be far greater than that of the channel entries. In such a case, the communication channel estimation task is to recover all the entries in \mathbf{H}_c . In mm-wave and THz bands with much fewer propagation paths than antennas, the mMIMO channel is well characterized by a geometrical clustered model, such as the Saleh–Valenzuela model, which enables beam space SP for mm-wave and THz communications that mimics MIMO radar SP. In fact, beam training and tracking in mm-wave and THz communications may be analogously viewed as target searching and tracking, all of which can be operated on a hybrid array-based RF platform. This also builds a solid foundation to merge R&C into a single system by ISAC technologies.

ISAC: The road from separation to integration

ISAC: From competitive coexistence to codesign

The ubiquitous deployment of R&C systems leads to severe competition over various resource domains. To date, both technologies exhibit explosively growing demands for spectral and spatial resources and are thus evolving toward higher frequencies and larger antenna arrays. As exemplified in the “Spectrum Characteristics and Management” section, a variety of R&C systems have to cohabitate within multiple frequency bands, which, inevitably, incurs significant mutual interference between the two functionalities [31], [34]. To ensure harmonious coexistence between R&C, orthogonal resource allocation became a viable approach. Nevertheless, orthogonal allocation results in low resource efficiency for both R&C. Aiming for

fully maximizing the potential of limited wireless resources, e.g., bandwidth, and to enable the codesign of the R&C functionalities, ISAC was proposed as a key technology for both next-generation wireless networks and radar systems.

The technological vision of ISAC can be divided into four levels, as shown in Figure 4. The first level is to share spectral resources between individual R&C systems, without interfering with each other. At the second level, the R&C functionalities may be deployed on the same hardware platform. At the third level, wireless resources may be fully reused between R&C via a common waveform, a single transmitting device, and a unified SP framework. Finally, at the fourth level, both R&C can share a common networking infrastructure, constructing a perceptive network to serve both sensing and communications functionalities. This underpins a large number of emerging IoT, 5G Advanced, and 6G applications that require high-quality communication, sensing, and localization services [5].

During the past three decades, the development of ISAC has been supported by a number of governmental projects worldwide, among which the most influential ones were the “Advanced Multifunction Radio Frequency Concept (AMRFC)” program initiated by the U.S. Office of Naval Research in the 1990s and the “Shared Spectrum Access for Radar and Communications (SSPARC)” project funded by DARPA in the 2010s [6]. While both projects were motivated by the need for sharing resources between R&C, the AMRFC mainly focused on colocating multifunctional modules (radar, communications, and electronic warfare) on the same RF front ends, and the SSPARC aimed for releasing part of the sub-6-GHz spectrum from the radar bands for shared use between R&C. Most of the technical outcome of these projects was used in formulating the level 1 to level 3 ISAC approaches. In the 2020s, networked sensing (level 4 ISAC) was recognized by major enterprises in the communications industry (Huawei, Ericsson, ZTE, Intel, and Nokia) as one of the core air interface technologies for Wi-Fi 7, 5G Advanced, and 6G [5]. In 2020, IEEE 802.11 formed the 802.11bf task

group to realize WLAN sensing in Wi-Fi 7, which is expected to be commercialized in 2024 [35]. In 2022, the 3rd Generation Partnership Project (3GPP) established the first study item on ISAC toward Release 19 standards for 5G Advanced [36].

To fully realize the promise of the ISAC technology, advanced SP techniques are indispensable. In this section, we

briefly review the recent research progress on the SP for ISAC. In particular, we focus on levels 3 and 4, where a unified signaling strategy is designed to serve the dual purposes of R&C.

ISAC signal processing

We investigate the linear Gaussian models considered in the “Fundamentals of Radar and Communications” section. The only

difference is that a unified ISAC signal \mathbf{S} is employed for both R&C, leading to

$$\begin{aligned} \text{Radar signal model: } \mathbf{Y}_r &= \mathbf{H}_r(\boldsymbol{\eta})\mathbf{S} + \mathbf{Z}_r; \\ \text{communication signal model: } \mathbf{Y}_c &= \mathbf{H}_c\mathbf{S} + \mathbf{Z}_c \end{aligned} \quad (18)$$

where \mathbf{S} is a discrete representation of the ISAC signal. We highlight that (18) consists of abstractions for many existing ISAC models. That is, an ISAC Tx transmits a signal \mathbf{S} to communicate information while detecting targets. For radar sensing applications, the radar Rx observes \mathbf{Y}_r and wishes to extract an estimate of $\boldsymbol{\eta}$ with the knowledge of the reference waveform \mathbf{S} , which is known to both the ISAC Tx and radar Rx. For communication applications, on the other hand, the communication Rx observes \mathbf{Y}_c and wishes to recover \mathbf{S} , which is unknown to the communication Rx.

A generic ISAC SP framework is presented in Figure 5, where the R&C functionalities are jointly coordinated at the ISAC Tx to form a baseband ISAC signal. After being upconverted to the RF band, the signal propagates through the R&C channels and arrives at the Rx. The received signal, which may consist of both target and communication information, first goes through a preprocessing procedure,

including synchronization, separation, filtering, and transformation, and is then processed following the regular R&C SP pipelines. ISAC SP is rather different from individual R&C SP. That is, when the wireless resources are shared between R&C, there exists an intrinsic performance tradeoff, as their design objectives are distinct and even contradictory. As illustrated in Figure 6, such a tradeoff can be framed as the Pareto frontier in terms of different R&C performance metrics, e.g., the radar’s CRB and communication rate. The complete characterization of such a Pareto

A variety of R&C systems have to cohabitate within multiple frequency bands, which, inevitably, incurs significant mutual interference between the two functionalities.

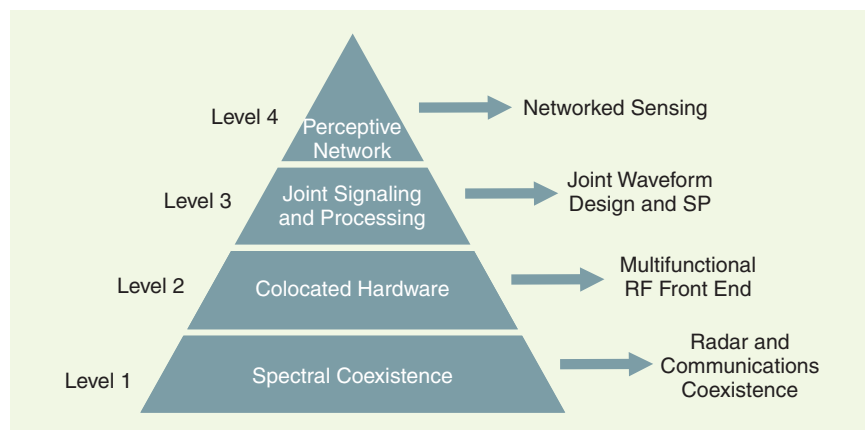


FIGURE 4. The evolution path for ISAC technologies.

frontier still remains wide open. The two corner points, P_{CS} and P_{SC} , represent the communication-optimal and radar-optimal performance, with the corresponding achievable rate–CRB pairs denoted by (C_{CS}, ϵ_{CS}) and (C_{SC}, ϵ_{SC}) , respectively. This results in three categories of ISAC SP designs, i.e., communication-centric, radar-centric, and joint design, which target approaching the points P_{CS} , P_{SC} and the Pareto frontier in between, respectively.

Communication-centric design

Communication-centric design (CCD) simply implements the radar sensing functionality over an existing and even commercialized communication waveform, in which case the communication functionality has priority. The most representative CCD approach is OFDM-based ISAC signaling, which directly exploits the OFDM communication waveform to simultaneously accomplish R&C tasks [20], [37]. Assume that the ISAC Tx emits the OFDM signal to communicate with a user while sensing a point target with delay τ and Doppler ν . After receiving the echo signal reflected from the target, the radar Rx, which is colocated with the ISAC Tx, samples at each OFDM symbol, followed by block-wise FFT processing. The resultant discrete signal can be arranged into a matrix, with its (n, m) th entry associating with the n th symbol at the m th subcarrier, given as

$$y_{n,m} = \alpha_{n,m} x_{n,m} e^{-j2\pi(m-1)\Delta f\tau} e^{j2\pi\nu(n-1)T_c} + z_{n,m} \quad (19)$$

where $\alpha_{n,m}$ and $z_{n,m}$ are the channel coefficient and noise. The random communication data $x_{n,m}$ impose a negative impact on radar sensing, which can be simply mitigated by element-wise division:

$$\begin{aligned} \tilde{y}_{n,m} &= \frac{y_{n,m}}{x_{n,m}} \\ &= \alpha_{n,m} e^{-j2\pi(m-1)\Delta f\tau} e^{j2\pi\nu(n-1)T_c} + \frac{z_{n,m}}{x_{n,m}}. \end{aligned} \quad (20)$$

Then, a 2D FFT can be applied to (20) to get the DD profile of the target.

Radar-centric design

In contrast to CCD schemes, radar-centric design (RCD) aims at implementing communication capability over existing radar infrastructures, targeting approaching the performance at P_{SC} . Since the classical radar waveform contains no information, RCD schemes are also referred to as *information embedding approaches* in the literature; namely, the communication data are embedded into the radar waveform in a way that will not unduly degrade the sensing performance. Early RCD schemes mainly focused on exploiting the LFM signal as an information carrier [38]. In addition to the conventional modulation formats, including amplitude, phase, and FSKs, LFM signals have another design DoF, i.e., the slope that the frequency increases with the time, which may also be utilized for data embedding. To fully guarantee the radar performance, recent research proposed to realize

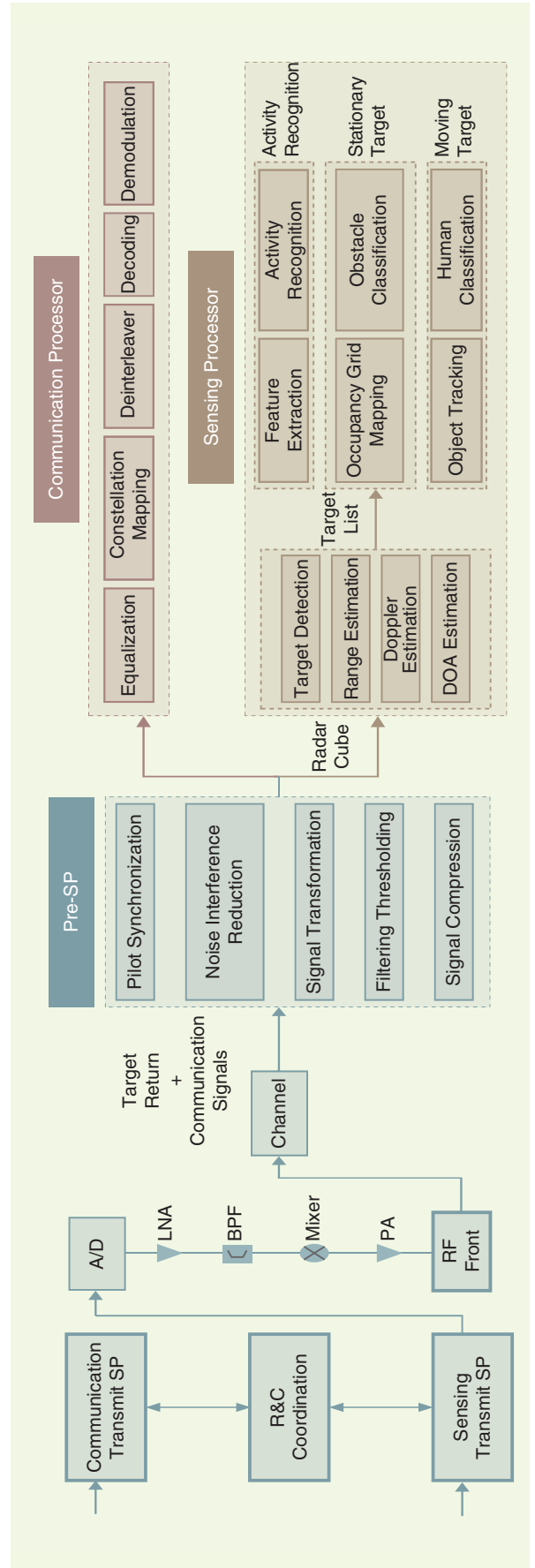


FIGURE 5. The general SP framework for ISAC systems. A/D: analog–digital; LNA: low-noise amplifier; BPF: bandpass filter; PA: power amplifier.

ISAC by index modulation (IM), which was first proposed in [39] for MIMO radar transmitting orthogonal waveforms. In such a case, the communication information is conveyed by shuffling the waveforms across multiple antennas, which does not break the orthogonality. As a step forward, more recent RCD schemes implement IM-based ISAC signaling on carrier-agile phased-array radar, namely, the multicarrier-agile joint radar–communication (MAJoRCom) system [40]. During each PRI, the MAJoRCom randomly selects the carrier frequencies from a frequency set and randomly allocates these frequencies to each antenna, which again keeps the orthogonality unaffected.

Joint design

As discussed in the preceding, CCD and RCD schemes attempt to approach the performance of P_{CS} and P_{SC} , which may be implemented in existing communication and radar systems, respectively. However, they lack the flexibility to formulate a scalable tradeoff between R&C and, equivalently, to approach the performance of an arbitrary point on the Pareto frontier in Figure 6. To resolve this issue, JD-based ISAC signaling becomes a promising strategy, which is often conceived through convex optimization techniques [41]. Consider a MIMO ISAC BS that serves K_u single-antenna users while detecting a point target locating at an angle θ . An ISAC signal \mathbf{S} constrained by the energy E_T can be obtained by solving the following angle CRB minimization problem under the sum–rate constraint:

$$\min_{\mathbf{S}} \text{CRB}(\theta) \quad \text{s.t.} \quad \sum_{k=1}^{K_u} R_k \geq R_0, \forall k, \|\mathbf{S}\|_F^2 \leq E_T \quad (21)$$

where R_k is the achievable rate for the k th user and R_0 is a pre-defined sum–rate threshold. The Pareto frontier between R&C can be obtained by increasing R_0 , which leads to an increased objective CRB.

Interplay between radar and communications

From the preceding ISAC SP strategies, it is interesting to note that there is a twofold tradeoff between R&C, namely, the deterministic versus random tradeoff (DRT) and subspace tradeoff (ST).

Deterministic-random tradeoff

Communication systems require random signals to convey as much information as possible, whereas radar systems prefer deterministic signals for achieving stable sensing performance. This has been an intuitive insight consistent with both engineers’ experience and R&C SP theory. For instance, constellation shaping for communications always targets approximating a Gaussian distribution, thus approaching the Shannon capacity. Radar systems, on the other hand, prefer to transmit constant-modulus waveforms at the maximum available power budget, which motivates the use of phase-coded signals. For clarity, this concept is shown in Figure 6.

The DRT has also been reflected in the preceding CCD and RCD approaches. For OFDM-based CCD signaling, the element-wise division of the random data changes the statistical characteristics of the noise across the symbols and subcarriers, imposing performance loss on the thresholding and peak detection in the 2D FFT processing. To tackle this issue, a natural idea is to transmit PSK-modulated data, which rotates the phase of the circularly symmetric Gaussian noise without changing its distribution. For the IM-based RCD scheme, the radar transmits communication data by the random selections of waveforms across the antennas, i.e., the information is carried by permutation and selection matrices, while keeping the radar waveform orthogonality unchanged. In both cases, the communication rate can be increased by embedding more random data (exploiting more DoFs) into the ISAC signal, which is, however, at the price of deteriorated radar sensing performance.

Subspace tradeoff

Another fundamental tradeoff in ISAC is the ST. The column vectors of R&C channel matrices \mathbf{H}_r and \mathbf{H}_c span the sensing and communication subspaces. To fully radiate the transmit power toward targets/users, radar-optimal and communication-optimal signals should align to the two subspaces, respectively. Consequently, the R&C performance can be balanced in an ISAC system by allocating resources into the two subspaces. Apparently, if two subspaces are partially overlapped, then resources allocated to the intersection are shared between R&C, improving the efficiency. On the contrary, if two subspaces are orthogonal to each other, no resources can be reused, leading

to zero performance gain. Based on the overlapped degree of two subspaces, one may categorize R&C channels as weakly coupled, moderately coupled, and strongly coupled scenarios, which are intuitively illustrated in Figure 7. The higher coupling degree between two subspaces results in better tradeoff performance, as more resources are reused between R&C.

The ST can be observed in the JD signaling scheme discussed in (21). That is, by increasing the communication sum–rate threshold R_0 , more

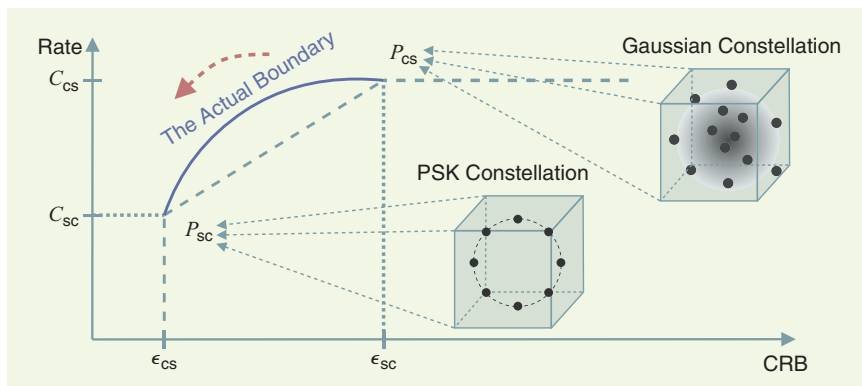


FIGURE 6. The performance tradeoff between R&C.

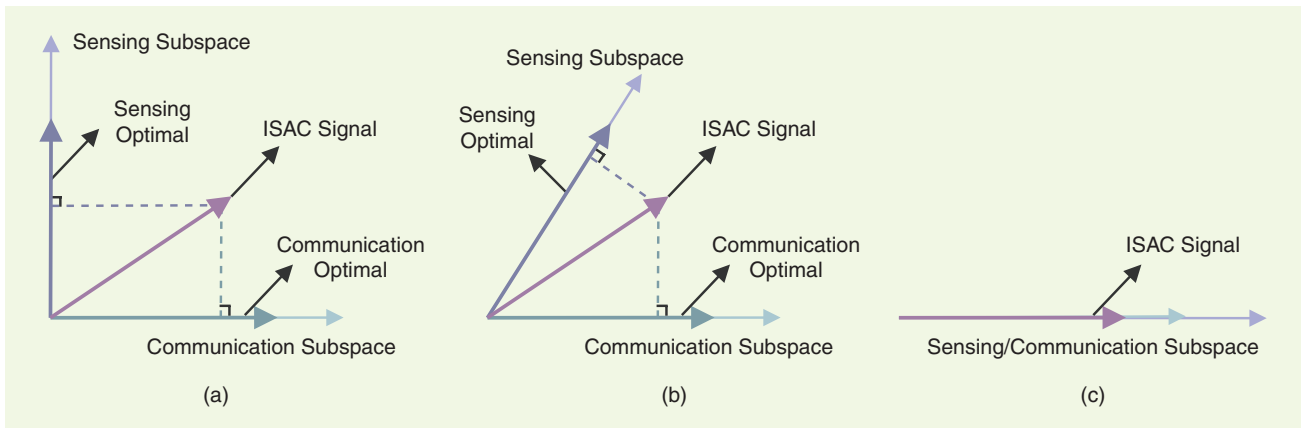


FIGURE 7. The ST and coupling effect in ISAC systems: (a) weakly coupled, (b) moderately coupled, and (c) strongly coupled.

signal power is transmitted toward the directions of communication users, while less power is radiated to sense the target, resulting in a higher CRB. To illustrate this, we provide a numerical example of solving problem (21) in Figure 8 for a single-target, single-user scenario. In particular, we consider the correlation coefficient between the communication channel \mathbf{h}_c and the target steering vector $\mathbf{a}(\theta)$, defined as $\rho = (\|\mathbf{h}_c^H \mathbf{a}(\theta)\|) / (\|\mathbf{h}_c\| \|\mathbf{a}(\theta)\|)$. By varying the signal-to-interference-plus-noise constraint of the user, we observe that the resultant ISAC signal indeed formulates a scalable tradeoff between the radar CRB and the communication achievable rate, where the ISAC signal rotates from the communication subspace to the sensing subspace. More interestingly, by increasing the correlation coefficient ρ from zero to one, the ISAC tradeoff performance becomes better, which is consistent with our analysis on weakly, moderately, and strongly correlated subspaces. That is, higher correlation between two subspaces indicates that more resources can be shared between R&C. In the extreme case of $\rho = 1$, the performance of both R&C reaches its optimum without jeopardizing one another. This is because the two subspaces are fully aligned to each other, and the signal resources can be fully reused between R&C, leading to the maximum gain.

Open challenges and future research directions

Although ISAC has been well investigated from various direction in recent years, there are still many open challenges that remain widely unexplored. Here, we overview some of the open problems in fundamental tradeoff, SP, and networking aspects, where tremendous research efforts are needed.

Full characterization of the ISAC performance tradeoff

Characterizing the ISAC performance tradeoff is a multiobjective functional optimization problem by its nature. Nevertheless, the current results are able to depict only the performance at the two corner points [42]. It is unclear where the exact Pareto frontier lies in Figure 6 and what the optimal signaling strategies are to achieve that boundary. Moreover, the research on the fundamental ISAC tradeoff in more practical scenarios, e.g., the multiuser multitarget regime, is still at its early stage,

where tighter estimation-theoretical bounds and the multiuser capacity region need to be jointly considered.

Practical ISAC signal processing

Most of the current ISAC signaling schemes were proposed under ideal assumptions. However, there is a large number of practical constraints that prevent the implementation of these ISAC designs. For instance, CCD approaches that adopt a standardized communication waveform, e.g., 5G New Radio, face the challenges of insufficient bandwidth and a high peak-to-average-power ratio, which leads to severe performance loss of radar sensing. In addition to that, the imperfection of hardware components, e.g., quantized phase shifters and uncalibrated antenna arrays, also needs to be taken into account in designing practical ISAC SP pipelines.

Networked ISAC

Current state-of-the-art research mainly concentrates on the SP for single-node ISAC systems. To realize networked ISAC using commercialized networking infrastructures, which are not

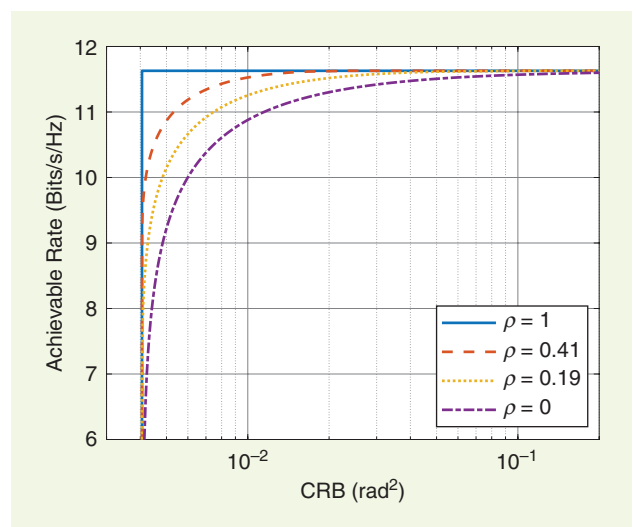


FIGURE 8. The R&C performance tradeoff under different correlation coefficients.

originally tailored for radar sensing, a series of SP challenges need to be carefully coped with. For instance, clock-level network synchronization is needed to achieve high sensing accuracy. Moreover, to detect short-range targets, e.g., humans and vehicles, the future ISAC BS should operate in full-duplex mode to avoid self-interference between the transmit signal and target return. Equipping the network with ubiquitous sensing capabilities has also raised concerns on security and privacy issues, which needs to be addressed in future ISAC systems.

Conclusions

In this article, we overviewed the technological evolution of R&C from an SP viewpoint. We first focused our discussion on the general principles and fundamental SP techniques for both R&C. We then introduced two main trends and the resulting SP schemes in the historical development of R&C, namely, the increase of frequencies and bandwidths and the expansion of the antenna arrays. Following these two trends, we provided a detailed discussion on the recent progress of SP techniques for ISAC systems. Finally, we identified a number of major open challenges in ISAC technologies.

Although concerning two long-established disciplines, the story of R&C will continue in the foreseeable future. In particular, ISAC, the marriage between R&C, will have a large impact on modern society.

Acknowledgment

This work was supported, in part, by the National Natural Science Foundation of China (Grant 62101234), the Shenzhen Science and Technology Program (Grant 20220815100308002), the National Key R&D Program of China (Grants 2018YFE0202101, 2018YFE0202103), and Guangdong Pearl River Talent Project (Grant 2021QN02X128). Le Zheng is the corresponding author.

Authors

Fan Liu (liuf6@sustech.edu.cn) received his Ph.D. degree from Beijing Institute of Technology, China, in 2018. He is now an assistant professor at the Southern University of Science and Technology, Shenzhen 518055, China. He serves as the founding academic chair of the IEEE Communications Society (ComSoc) Integrated Sensing and Communications (ISAC) Emerging Technology Initiative, an associate editor of *IEEE Communications Letters* and *IEEE Open Journal of Signal Processing*, and a founding member of the IEEE Signal Processing Society (SPS) ISAC Technical Working Group. He was a recipient of the 2023 ComSoc Stephan O. Rice Prize, 2021 SPS Young Author Best Paper Award, and 2019 Chinese Institute of Electronics Best Doctoral Thesis Award. His research interests include signal processing, wireless communications, and, in particular, ISAC. He is a Member of IEEE.

Le Zheng (le.zheng.cn@gmail.com) received his Ph.D. degree in 2015 from Beijing Institute of Technology, Beijing 100081, China, where he is now a professor with the School of Information and Electronics. He is a founding member of the IEEE Communications Society Integrated Sensing and

Communications (ISAC) Emerging Technology Initiative and a guest editor of *IEEE Journal of Selected Topics in Signal Processing* and *IEEE Wireless Communications*. His research interests include radar, statistical signal processing, wireless communication, and high-performance hardware, particularly in the area of automotive radar and ISAC. He is a Senior Member of IEEE.

Yuanhao Cui (cuiyh@sustech.edu.cn) received his Ph.D. degree from Beijing University of Posts and Telecommunications, China. He is now a research assistant professor at the Southern University of Science and Technology, Shenzhen 518055, China. He serves as the secretary and founding member of the IEEE Communications Society Integrated Sensing and Communications (ISAC) Emerging Technology Initiative. His research interests include precoding and protocol designs for ISAC. He is a Member of IEEE.

Christos Masouros (c.masouros@ucl.ac.uk) received his Ph.D. degree from the University of Manchester, U.K. He is currently a professor at University College London, WC1E 7JE London, U.K. He is an editor of *IEEE Transactions on Wireless Communications* and *IEEE Open Journal of Signal Processing*, an editor at large of *IEEE Open Journal of the Communications Society*, and a founding member and vice-chair of the IEEE Communications Society (ComSoc) Integrated Sensing and Communications (ISAC) Emerging Technology Initiative. He was the recipient of the 2023 IEEE ComSoc Stephen O. Rice Prize, corecipient of the 2021 IEEE Signal Processing Society Young Author Best Paper Award, and recipient of the 2019 IEEE Wireless Communications and Networking Conference Best Paper Award. His research interests include wireless communications and signal processing, with particular focus on green communications, large-scale antenna systems, ISAC, and interference mitigation techniques. He is a Senior Member of IEEE.

Athina P. Petropulu (athinap@rutgers.edu) received her Ph.D. degree from Northeastern University, Boston. She is a distinguished professor of electrical and computer engineering at Rutgers University, Rutgers, NJ 08854, USA. She is the president of the IEEE Signal Processing Society (SPS). She received the Presidential Faculty Fellow Award (1995) from the U.S. National Science Foundation and the White House and the 2012 SPS Meritorious Service Award. She is a coauthor of the 2005 IEEE Signal Processing Magazine Best Paper Award, 2020 SPS Young Author Best Paper Award (with B. Li), 2021 SPS Young Author Best Paper Award (with F. Liu), and 2021 IEEE Aerospace and Electronic Systems Society Barry Carlton Best Paper Award. Her research interests include radar signal processing and physical layer security. She is a Fellow of IEEE and the American Association for the Advancement of Science.

Hugh Griffiths (h.griffiths@ucl.ac.uk) received his Ph.D. and D.Sc. (Eng.) degrees in 2000 in electronic engineering from University College London, WC1E 7JE London, U.K., where he currently holds the Thales/Royal Academy of Engineering Chair of RF Sensors in the Department of Electronic and Electrical Engineering. His research interests include radar and

sonar systems, signal processing (particularly synthetic aperture radar and bistatic radar), and antenna measurement techniques. He is a Fellow of IEEE, the Institution of Engineering and Technology, and the Royal Academy of Engineering.

Yonina C. Eldar (yonina.eldar@weizmann.ac.il) received her Ph.D. degree in electrical engineering and computer science from the Massachusetts Institute of Technology (MIT) in 2002. She is a professor in the Department of Math and Computer Science, Weizmann Institute of Science, Rehovot 7610001, Israel, where she heads the center for Biomedical Engineering and Signal Processing. She is also a visiting professor at MIT, Cambridge, MA 02412 USA, and the MIT Broad Institute. She is a member of the Israel Academy of Sciences and Humanities and a fellow of the European Association for Signal Processing. She is the editor-in-chief of *Foundations and Trends in Signal Processing* and serves IEEE on several technical and award committees. She has received the IEEE Signal Processing Society Technical Achievement Award, IEEE Aerospace and Electronic Systems Society Fred Nathanson Memorial Radar Award, and IEEE Kiyo Tomiyasu Award. She is a Fellow of IEEE.

References

- [1] H. Griffiths, "Oliver Heaviside and the Heaviside layer," *Philos. Trans. Roy. Soc. A*, vol. 376, no. 2134, Oct. 2018, Art. no. 20170459, doi: 10.1098/rsta.2017.0459.
- [2] L. Yang and G. Giannakis, "Ultra-wideband communications: An idea whose time has come," *IEEE Signal Process. Mag.*, vol. 21, no. 6, pp. 26–54, Nov. 2004, doi: 10.1109/MSP.2004.1359140.
- [3] J. Li and P. Stoica, "MIMO radar with colocated antennas," *IEEE Signal Process. Mag.*, vol. 24, no. 5, pp. 106–114, Sep. 2007, doi: 10.1109/MSP.2007.904812.
- [4] T. L. Marzetta, "Noncooperative cellular wireless with unlimited numbers of base station antennas," *IEEE Trans. Wireless Commun.*, vol. 9, no. 11, pp. 3590–3600, Nov. 2010, doi: 10.1109/TWC.2010.092810.091092.
- [5] F. Liu et al., "Integrated sensing and communications: Toward dual-functional wireless networks for 6G and beyond," *IEEE J. Sel. Areas Commun.*, vol. 40, no. 6, pp. 1728–1767, Jun. 2022, doi: 10.1109/JSAC.2022.3156632.
- [6] F. Liu, C. Masouros, A. Petropulu, H. Griffiths, and L. Hanzo, "Joint radar and communication design: Applications, state-of-the-art, and the road ahead," *IEEE Trans. Commun.*, vol. 68, no. 6, pp. 3834–3862, Jun. 2020, doi: 10.1109/TCOMM.2020.2973976.
- [7] S. Kotz and N. L. Johnson, *Breakthroughs in Statistics: Foundations and Basic Theory*. New York, NY, USA: Springer Science & Business Media, 2012.
- [8] R. Schmidt, "Multiple emitter location and signal parameter estimation," in *Proc. RADC Spectr. Estimation Workshop*, Rome, NY, USA: Rome Air Development Center, Oct. 1979; reprinted in *IEEE Trans. Antennas Propag.*, vol. 34, pp. 276–280, Mar. 1986.
- [9] R. Roy and T. Kailath, "ESPRIT-estimation of signal parameters via rotational invariance techniques," *IEEE Trans. Acoust., Speech, Signal Process.*, vol. 37, no. 7, pp. 984–995, Jul. 1989, doi: 10.1109/29.32276.
- [10] C. E. Shannon, "A mathematical theory of communication," *Bell Syst. Tech. J.*, vol. 27, no. 3, pp. 379–423, Jul. 1948, doi: 10.1002/j.1538-7305.1948.tb01338.x.
- [11] P. Woodward, "Theory of radar information," *Trans. IRE Prof. Group Inf. Theory*, vol. 1, no. 1, pp. 108–113, Feb. 1953, doi: 10.1109/TIT.1953.1188560.
- [12] D. Guo, S. Shamai, and S. Verdú, "Mutual information and minimum mean-square error in Gaussian channels," *IEEE Trans. Inf. Theory*, vol. 51, no. 4, pp. 1261–1282, Apr. 2005, doi: 10.1109/TIT.2005.844072.
- [13] H. Griffiths et al., "Radar spectrum engineering and management: Technical and regulatory issues," *Proc. IEEE*, vol. 103, no. 1, pp. 85–102, Jan. 2015, doi: 10.1109/JPROC.2014.2365517.
- [14] N. Levanon and E. Mozeson, *Radar Signals*. Hoboken, NJ, USA: Wiley, 2004.
- [15] K. Rutenber and L. Chanzit, "High range resolution by means of pulse to pulse frequency shifting," in *Proc. IEEE Eascon Rec. Aerosp. Electron. Syst. Tech. Conv.*, 1968, pp. 47–51.
- [16] Y. C. Eldar and G. Kutyniok, *Compressed Sensing: Theory and Applications*. Cambridge, U.K.: Cambridge Univ. Press, 2012.
- [17] A. De Maio, Y. C. Eldar, and A. M. Haimovich, *Compressed Sensing in Radar Signal Processing*. Cambridge, U.K.: Cambridge Univ. Press, 2019.
- [18] M. Zimmerman and A. Kirsch, "The AN/GSC-10 (KATHRYN) variable rate data modem for HF radio," *IEEE Trans. Commun.*, vol. 15, no. 2, pp. 197–204, Apr. 1967, doi: 10.1109/TCOM.1967.1089577.
- [19] J. W. Cooley and J. W. Tukey, "An algorithm for the machine calculation of complex Fourier series," *Math. Comput.*, vol. 19, no. 90, pp. 297–301, Apr. 1965, doi: 10.1090/S0025-5718-1965-0178586-1.
- [20] C. Sturm and W. Wiesbeck, "Waveform design and signal processing aspects for fusion of wireless communications and radar sensing," *Proc. IEEE*, vol. 99, no. 7, pp. 1236–1259, Jul. 2011, doi: 10.1109/JPROC.2011.2131110.
- [21] R. Hadani and A. Monk, "OTFS: A new generation of modulation addressing the challenges of 5G," 2018, *arXiv:1802.02623*.
- [22] W. Yuan et al., "Integrated sensing and communication-assisted orthogonal time frequency space transmission for vehicular networks," *IEEE J. Sel. Topics Signal Process.*, vol. 15, no. 6, pp. 1515–1528, Oct. 2021, doi: 10.1109/JSTSP.2021.3117404.
- [23] P. Swerling, "Probability of detection for fluctuating targets," *IRE Trans. Inf. Theory*, vol. 6, no. 2, pp. 269–308, Apr. 1960, doi: 10.1109/TIT.1960.1057561.
- [24] A. J. Paulraj and T. Kailath, "Increasing capacity in wireless broadcast systems using distributed transmission/directional reception (DTDR)," U.S. Patent 5 345 599, Sep. 1994.
- [25] D. Bliss and K. Forsythe, "Multiple-input multiple-output (MIMO) radar and imaging: Degrees of freedom and resolution," in *Proc. Asilomar Conf. Signals Syst. Comput.*, 2003, vol. 1, pp. 54–59, doi: 10.1109/ACSSC.2003.1291865.
- [26] S. Fortunati, L. Sanguinetti, F. Gini, M. S. Greco, and B. Himed, "Massive MIMO radar for target detection," *IEEE Trans. Signal Process.*, vol. 68, pp. 859–871, Jan. 2020, doi: 10.1109/TSP.2020.2967181.
- [27] O. E. Ayach, S. Rajagopal, S. Abu-Surra, Z. Pi, and R. W. Heath, "Spatially sparse precoding in millimeter wave MIMO systems," *IEEE Trans. Wireless Commun.*, vol. 13, no. 3, pp. 1499–1513, Mar. 2014, doi: 10.1109/TWC.2014.011714.130846.
- [28] A. Hassaniien and S. A. Vorobyov, "Phased-MIMO radar: A tradeoff between phased-array and MIMO radars," *IEEE Trans. Signal Process.*, vol. 58, no. 6, pp. 3137–3151, Jun. 2010, doi: 10.1109/TSP.2010.2043976.
- [29] H. Q. Ngo, A. Ashikhmin, H. Yang, E. G. Larsson, and T. L. Marzetta, "Cell-free massive MIMO versus small cells," *IEEE Trans. Wireless Commun.*, vol. 16, no. 3, pp. 1834–1850, Mar. 2017, doi: 10.1109/TWC.2017.2655515.
- [30] A. M. Haimovich, R. S. Blum, and L. J. Cimini, "MIMO radar with widely separated antennas," *IEEE Signal Process. Mag.*, vol. 25, no. 1, pp. 116–129, 2008, doi: 10.1109/MSP.2008.4408448.
- [31] L. Zheng, M. Lops, Y. C. Eldar, and X. Wang, "Radar and communication coexistence: An overview: A review of recent methods," *IEEE Signal Process. Mag.*, vol. 36, no. 5, pp. 85–99, Sep. 2019, doi: 10.1109/MSP.2019.2907329.
- [32] Y. S. Cho, J. Kim, W. Y. Yang, and C. G. Kang, *MIMO-OFDM Wireless Communications with MATLAB*. Hoboken, NJ, USA: Wiley, 2010.
- [33] L. Zheng and D. Tse, "Diversity and multiplexing: A fundamental tradeoff in multiple-antenna channels," *IEEE Trans. Inf. Theory*, vol. 49, no. 5, pp. 1073–1096, May 2003, doi: 10.1109/TIT.2003.810646.
- [34] B. Li and A. P. Petropulu, "Joint transmit designs for coexistence of MIMO wireless communications and sparse sensing radars in clutter," *IEEE Trans. Aerosp. Electron. Syst.*, vol. 53, no. 6, pp. 2846–2864, Dec. 2017, doi: 10.1109/TAES.2017.2717518.
- [35] C. Chen et al., "Wi-Fi sensing based on IEEE 802.11bf," *IEEE Commun. Mag.*, vol. 61, no. 1, pp. 121–127, Jan. 2023, doi: 10.1109/MCOM.007.2200347.
- [36] "Study on integrated sensing and communication," 3rd Generation Partnership Project, Sophia Antipolis, France, Tech. Rep. 22.837, 2022.
- [37] M. F. Keskin, H. Wymeersch, and V. Koivunen, "MIMO-OFDM joint radar-communications: Is ICI friend or foe?" *IEEE J. Sel. Topics Signal Process.*, vol. 15, no. 6, pp. 1393–1408, Mar. 2021, doi: 10.1109/JSTSP.2021.3109431.
- [38] G. N. Saddik, R. S. Singh, and E. R. Brown, "Ultra-wideband multifunctional communications/radar system," *IEEE Trans. Microw. Theory Techn.*, vol. 55, no. 7, pp. 1431–1437, Jul. 2007, doi: 10.1109/TMTT.2007.900343.
- [39] E. BouDaher, A. Hassaniien, E. Aboutanios, and M. G. Amin, "Towards a dual-function MIMO radar-communication system," in *Proc. IEEE Radar Conf. (RadarConf)*, May 2016, pp. 1–6, doi: 10.1109/RADAR.2016.7485316.
- [40] T. Huang, N. Shlezinger, X. Xu, Y. Liu, and Y. C. Eldar, "MAJoRCOM: A dual-function radar communication system using index modulation," *IEEE Trans. Signal Process.*, vol. 68, pp. 3423–3438, May 2020, doi: 10.1109/TSP.2020.2994394.
- [41] F. Liu, Y.-F. Liu, A. Li, C. Masouros, and Y. C. Eldar, "Cramér-Rao bound optimization for joint radar-communication beamforming," *IEEE Trans. Signal Process.*, vol. 70, pp. 240–253, Jan. 2022, doi: 10.1109/TSP.2021.3135692.
- [42] Y. Xiong, F. Liu, Y. Cui, W. Yuan, and T. X. Han, "Flowing the information from Shannon to Fisher: Towards the fundamental tradeoff in ISAC," in *Proc. IEEE Global Commun. Conf. (GLOBECOM)*, Dec. 2022, pp. 1–6.